Impact of new seismic parameters on earthquake scenario based on Geospatial Information System

Sadra KARIMZADEH[1*], Masakatsu MIYAJIMA[2], Reza HASSANZADEH[3], Reza AMIRASLANZADEH[4], Batoul KAMEL[5]

[1]Member of JSCE, Faculty of Environmental Design, Kanazawa University
*E-mail: sadra.karimzadeh@gmail.com

[2]Member of JSCE, Professor, Faculty of Environmental Design, Kanazawa University, Japan

[3] School of Geography, Planning and Environmental Policy, University College Dublin (UCD), Ireland

[4]Member of JSCE, Faculty of Environmental Design, Kanazawa University, Japan

[5]Faculty of Geography, University of Tabriz, Iran

Abstract

This paper presents a new integrated model consisting geological, geodetical, geotechnical and geophysical parameters to create a multi-parameter seismic microzonation map. An integrated GIS-oriented model such as this work will be able to partially illuminate consequences of a possible earthquake. Therefore, it creates an opportunity for managers and decision-makers to revise the existing plans, and also to consider all factors in future urban extension plans. An evaluation of structural damages, population vulnerability and post-earthquake demands based on previous earthquake reports is carried out for district two in Tabriz city, Iran. This district has around 16.53 km^2 under-construction and dwelling area with an incredible growing trend along the North Tabriz Fault which is a distinguished tectonic structure in the vicinity of the city. Results show that 69.5% of existing buildings are destroyed totally and the rate of fatalities is about 33% after a scenario of 7 magnitude earthquake occurrence.

Key Words : *Seismic microzonation; GIS-oriented; Vulnerability; North Tabriz Fault*

1. INTRODUCTION

One of the basic necessities of disaster management of cities during (co-), after (post-) or even before (pre-) an earthquake is providing a well-enriched geodatabase. The existence of such database helps engineers, urban planners, to predict what will happen in the future; therefore they can make better strategies about the future of cities. Spatial-based earthquake scenarios in order to plan for quick responses is a basis for urban preparation and earthquake disaster management using decision making techniques. We know that insecure structures, inadequate studies of earthquake scenarios, inefficient crisis management and unforeseen risks after an earthquake (i.e. induced landslides, broken water and gas pipes, interruption of power transmission and telecommunication facilities) are the reasons of losses in Iran where thousands of faults are located in the vicinity of cities[2]. These faults are able to generate unpredictable earthquakes during time and location.

Disasters occurrence such as earthquakes, floods, and fires, have a huge effect on the community and infrastructures. Most natural phenomena are characterized by short action but their impacts for example on buildings or other tangible structures last for years. The presented analytical risk models enhance the ability and resilience of experts and urban planners against natural disasters. A glimpse on the hazard-damage assessment models shows that each the models use specific parameters and formulation approach and can be categorized in two main classes: (1) worldwide models and (2) local (case-based) models. A principal example for the first category is Prompt

Assessment of Global Earthquake for Response (PAGER) operated by USGS, reports economic losses and estimation of people exposed to varying levels of ground shaking. It is able to give a report within 30 minutes after a significant earthquake (usually for events greater than magnitude 5.5) [3]. However information on the extend shaking are not accurate in the first hours after an earthquake due to spatial variability of ground motion and typically improves using seismic data and intensity reports (for details see [3-5]). For the second category, HAzards United States (HAZUS) is a multi-hazard model in three main natural disasters in US such as earthquake, wind and flood which was developed by Federal Emergency Management Agency (FEMA) [6,7]. It works on Arc Map interface and estimates physical damages (i.e. buildings, pipeline networks) and social damage (i.e. casualties) based on damage functions and census tract areas, respectively. It has been used for pre-disaster mitigation of most counties of United States such as: Yuba in California, Harris in Texas, etc. [8,9]. Çinicioğlu et al.[10] presented an integrated damage-causing model including (1) ground shaking as primary effect (2) landslide, liquefaction and seismic bearing capacity as collateral effects. This method considered each effective phenomenon separately and in combination for two districts, Bakırköy and Ömerli, in Istanbul city. Ansal et al. [11] presented a seismic microzonation and earthquake damage scenario for Zeytinburnu in Istanbul. They firstly generated different microzonation maps with respect to ground shaking parameters (i.e. fault orientation, magnitude, fault geometry) due to the selected earthquake scenario. In order to evaluate seismic vulnerability for buildings, they calculated site-specific short period (T=0.2) and long period (T=1) spectral accelerations and PGAs. Secondly, region-specific vulnerability curves were used to estimate building damage in Zeytinburnu. Thirdly, natural gas pipeline damage was estimated by empirical correlations (PGV vs. pipeline damage) and gas pipeline inventories. Armaş [12] presented a multi-criteria vulnerability assessment to earthquake model of Bucharest city in Romania which uses a bunch of raster indicators. Each indicator (i.e. acceleration value of an earthquake and/or population) provided spatial information on set of defined criteria (i.e. environmental or social vulnerability). It is processed and classified in "criteria trees" according to their weight to vulnerability. Cole et al. [13] estimated rate of expected building damage in three quarters of Shanghai in China using attenuation Gumbel relationships and building damage factor. Hashemi and Alesheikh [14] modified intensity of earthquake to investigate impacts of ground shaking on building damages, population vulnerability and street blockage in district 10 of Tehran metropolitan, Iran. Hassanzadeh et al. [2] presented a user-friendly Karmania Hazard Model (KHM) to Kerman city in Iran. KHM has an interactive environment which combines spatial data layers and vulnerability coefficient of buildings and population to estimate rate of building damages, causalities and required resources for survivors and injured people. It was conceptualized and developed by a group of researchers in Kerman Disaster Management Center (KDMC) and was validated with Bam earthquake on (1) Seismic intensity, (2) Rate of damaged buildings and number of death people, (3) Report of post-earthquake demands. In this paper, ArcGIS package enables us to turn parameters into actionable information. All parameters, such as geological characteristics, predominant period of soil and shear wave velocity, geoid gradient, types of sediment, alluvial thickness and ground water table are converted to shape files, classified and finally integrated in a relational geodatabase to evaluate damage of structures and rate of fatalities and injuries in district two of Tabriz city. Then we present post-earthquake demands of the study area. The results show that 69.5% of buildings destructed totally and the rate of fatalities is about 33% .

2. SEISMICITY OF STUDY AREA

Tabriz metropolitan with a population over 1.5 million people is comprised of 10 regions. In terms of land area, it is the second large city of Iran which contains about 25 km^2 old texture [1]. The city developed between Eynali and Sahand mountains in North and South, respectively. According to the topography of the study area, slope slightly decreases from east to west and opens to Tabriz basin. The city, capital of Eastern-Azerbaijan province is situated in NW Iran at 38.08ºN, 46.25ºE. GPS constrains and earthquake focal solutions of past earthquakes in NW Iran that were performed by Jackson 1992 [15] and McClusky et al. [16] indicate that the convergence of 22±2 mm/yr between northward motion of Arabia plate relative to Eurasia plate causes the emergence of numerous thrust and strike-slip faults in this region (Fig. 1).

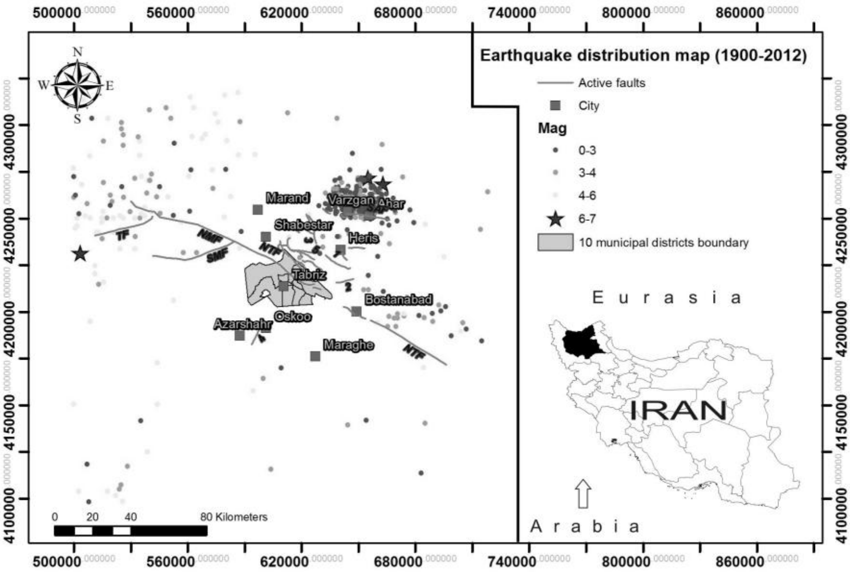

Fig1. Summary structural map of East-Azerbaijan province of Iran adopted from Hessami et al. [21]. Seismicity is from Berberian [22], Centroid Moment Tensor (http://www.globalcmt.org/) and International Institute of Earthquake Engineering and Seismology (http://www.iiees.ac.ir) catalogues between 1900-2012. North Tabriz Fault (NTF); South Misho Fault (SMF); North Misho Fault (NMF); Tasuj Fault (TF); and South Ahar Fault (SAF).

Westaway [17] and Jackson [15] believe that strike-slips faults (i.e. North Tabriz Fault, Gila-tu-Siyah Cheshmeh-Khoy Fault and Chalderan Fault) appear to be continuation of the North Anatolian Fault into NW Iran. Some of these fault segments were ruptured during 1930, 1966 and 1976 earthquakes and trailed surface deformations [17-20]. Last major earthquakes caused by North Tabriz Fault (NTF) in 18th century are as follows: The first one happened in 1721 (Ms 7.3) at 37.9ºN, 46.7ºE, and the second one happened in 1780 (Ms 7.4) at 38.12ºN, 46.29ºE [22]. Location and elapse of time relate a high seismic region for both SE and NW segments of North Tabriz Fault. However initial seismic hazard assessment needs an estimated value of potential earthquake in a specific area causing by a specific fault. The maximum magnitude and perceivable intensity in Tabriz for dataset of faults are calculated by different empirical equations and summarized in Table 1. Due to the length of the fault and adjacency to the site, the NW segment of the NTF poses more seismic hazard. Moreover, time series analysis of RADAR images in the study area between 2004-2010 supports a probable earthquake with Mw ~ 7 as a result of strain accumulation across the North Tabriz Fault [23]. The average thickness of lithosphere is estimated from gravimetric measurements to be about 40 km for NW Iran [24]. Statistical results of instrumental earthquake catalogues in NW Iran with a radius of 150 km indicate that seismogenic depth is about 20 km and the numbers of recorded events in day-time are less than night-time earthquakes [25]. Because of poor instrumental records of smaller events in the recent decades, the magnitude of most earthquakes in this radius is in range of M 4 to M 4.5. There is no evidence for increasing trend of M 4 to M 4.5 earthquakes during the time. It is in conflict with the Gutenberg-Richter law which confirms that smaller events have not recorded well [25]. The last seismic event of the study area happened on 11th August 2012 in Ahar region, NW Iran. The epicenter of the earthquakes was 60 km far from Tabriz city. The felt intensity degree in Tabriz was V (MMI), and the group of aftershocks continued for eight months (Fig. 1).

3. METHODOLOGY

Estimation of seismic hazard risk for different parts of the world takes a different methods and parameters. The database could affect other steps of seismic microzonation, therefore there is not a standard approach of damage assessment so far. This paper benefits a relational geodatabase for query and calculation which all data is represented in terms of tuples, grouped into relations. We attempt to increase the number of new parameters which are effective in Iran seismic zone. Consequently, for a hierarchy process approach, each parameter takes a specific weight which comes out from expert judgments. We use the KHM standard method which is designed for Iran and

Table 1 Seismic parameters of distinguished faults of the study area (see Fig. 1 for their location)

Fault name	Length (km)	Magnitude of possible earthquake				Average magnitude	Perceivable MMI in Tabriz
		Nowroozi [26]	Wells and Coppersmith [27]	Mohajer and Nowroozi [28]	Bonilla et al. [29]		
NW-NTF	45	6.64	6.99	7.03	7.58	7.06	IX
SE-NTF	46.5	6.69	7.03	7.06	7.63	7.1	VII
SMF	45	6.68	7.02	7.05	7.63	7.09	VIII
NMF	42	6.63	6.98	7.02	7.56	7.04	VII
TF	32.5	6.49	6.84	6.91	7.3	6.89	VI
SAF	40	6.5	6.7	6.45	6.7	6.56	VII
1	14	6.01	6.30	6.5	6.64	6.36	VII
2	9.5	5.8	6.19	6.37	6.34	6.2	VII
3	15.3	6.07	6.44	6.58	6.71	6.45	VII
4	13.2	6.01	6.36	6.52	6.6	6.37	VII
5	10.2	5.87	6.23	6.4	6.4	6.22	VII

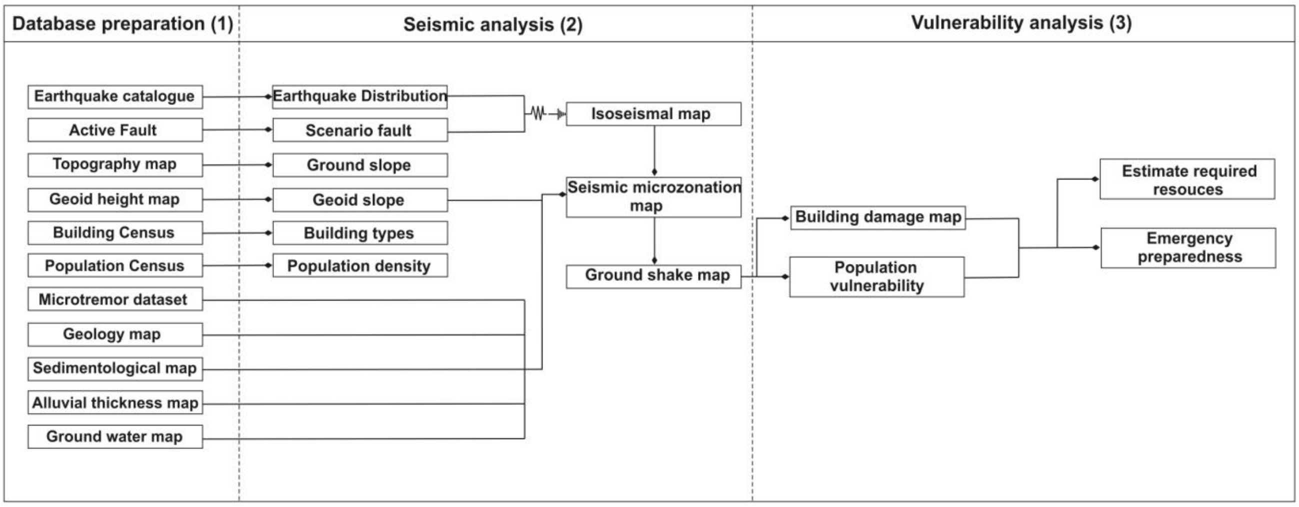

Fig 2. Flow chart of earthquake scenario model.

then we extrude a 3D scene of demolished buildings. Based on a GIS-upholded database, the principal tasks of presented earthquake scenario can be followed in 3 steps (Fig. 2).

(1) Data preparation

At this stage, data with different characteristics are gathered and adopted in order to be utilized in ArcGIS environment. An earthquake catalogue was obtained from International Institute of Earthquake Engineering and Seismology (IIEES), then it is modified with first earthquake catalogue [22]. The modified catalogue is tabulated with geographic coordinate, depth (km) and earthquake magnitude within year/month/day format. The geology map is provided by Geological Survey of Iran (GSI) at the scale of 1:100000. It shows the NW Iran is well-known with various lithologies and ages [30]. Residential districts of Tabriz contain the Cenozoic and Quaternary units. The Cenozoic units last from Miocene to Quaternary. Younger terraces, gravel fan, and salty-gypsiferous lay on residential parts of our target district (Fig. 3a) [30,31]. The ASTER digital elevation model (30 m posting) has been used in order to evaluate terrain slope (Fig. 3b). Tabriz region starts with a gentle slope from the east to the west. Elevations vary from 1750 m in the east to 1300 m in the west. The average height of topography in district two is estimated to be about 1500 m. Geoid slope map is another parameter of seismic microzoning project of Tabriz which comes out from geoid map (Fig. 3c). It is prepared by International Center for Global Earth Models (ICGEM). The geoid simply stated, is the fundamental surface that describes figure of Earth. It can be described as the equi-potential surface of Earth's gravity filed. Geoid value of NW Iran is in the range of 15-25 m. The last Integrated investigation of seismology data and geoid gradient of Iran, reveals a

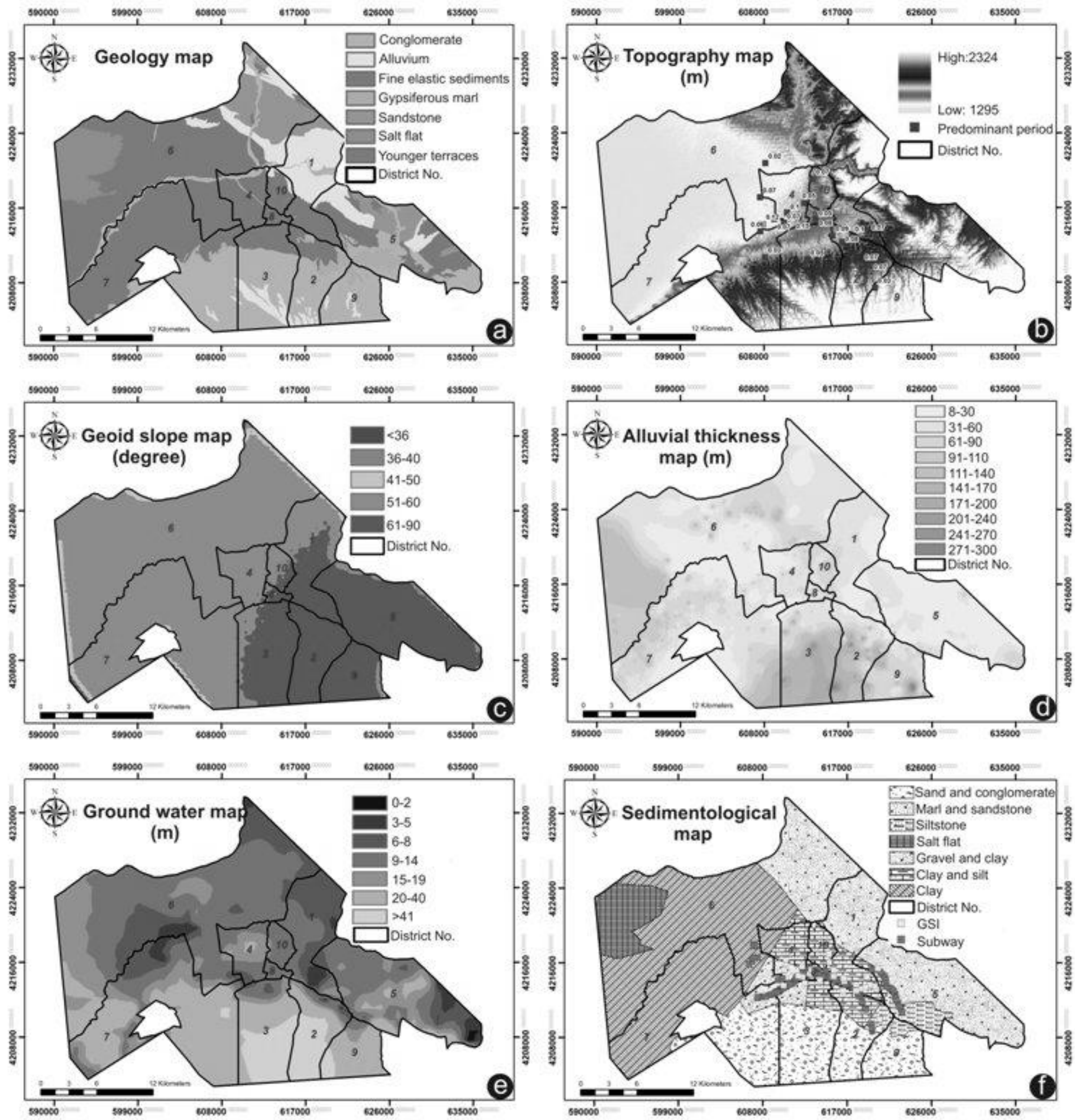

Fig. 3. Effective local factors in ten municipality's region of Tabriz city.

significant spatial correlation between place of past earthquakes and geoid slope which all Iranian earthquakes with magnitude greater than 6 are located in areas with a higher geoid slope exceeding 7.5% [32,33].

Alluvial thickness and ground water table of Tabriz were provided through Regional Water Organization in X,Y, and Z format (Fig. 3 d and e). In order to realize this fact that how soil condition could amplify earthquake waves, we use shear wave velocity and microtremor measurements of 21 stations in different parts of Tabriz (Fig. 3e) to categorize soil types based on table 2 [34]. Sedimentology map extracted from geotechnical studies of GSI and also exploration studies of subway project in the city [30,31,35]. Overall 149 boreholes and shallow wells were excavated in the study area (Fig. 3f). Average depth of boreholes is about 30 m. In order to study compressibility of subsurface layers, some tests were done, such as Standard Penetration Test (SPT) and pressuremeter test. According to the drilling results surface layers are mostly alluvial deposits, in some boreholes weak stone layers such as: siltstone, clay stone and conglomerate are dominant [31].

(2) Seismic analysis

As discussed, North Tabriz Fault (NTF) is a prominent tectonic feature in the vicinity of the city. A future earthquake on each segment of NTF would have a significant impact on buildings and population in Tabriz city, as Table 1 shows the seismic activity of this fault also high.

Table 2 Soil profile classification based on Iranian Code of Practice for Seismic Resistant Design of Buildings: Standard No. 2800 [36].

Soil type	Description	V_s(m/sec)
I	a) Igneous rock (with coarse and fine grade texture), stiff sedimentary rocks and massive metamorphic rocks and conglomerate. b) Stiff soils (compact sand and gravel, very stiff clay) with a thickness more than 30 m above the bedrock.	> 750 $375 \leq V_s \leq 750$
II	a) Loose igneous rocks (i.e. tuff), loose sedimentary rocks, foliated metamorphic rocks and in general rocks that have become loose and decomposed due to weathering b) Stiff soils (compact sand and gravel, very stiff clay) having a thickness more than 30 m above the bedrock.	$375 \leq V_s \leq 750$ $375 \leq V_s \leq 750$
III	a) Rocks that are disintegrated due to weathering. b) Soils with medium compaction, layers of sand and gravel with medium intra-granular bond and clay with intermediate compaction.	$175 \leq V_s \leq 375$ $175 \leq V_s \leq 375$
IV	a) Soft deposits with high moisture content due to high level of water table. b) Any soil profile containing clay with a minimum thickness of 6 m and a plastic index and moisture content exceeding 20 and 40 percent, respectively.	<175

Two major factors in order to develop a worst-case seismic scenario are: the length of fault and proximity to the residential areas. Therefore the NW segment of NTF is selected to simulate the probable earthquake. The initial elements of hypothesized fault are summarized in table 3. An optional hazard risk approach is simulated based on Seismic Rehabilitation of Existing Buildings code (SREB) [37]. The attenuation of ground motion (intensity-MMI), that is the severity at which the earthquake is felt in a particular place. It becomes less intense in further distance from the epicenter. We use region-specific intensity attenuation relationships which arise from major Iranian earthquakes (22 earthquakes in different parts of Iran) to produce isoseismal map (Eq. 1, 2) (Fig. 4a) [38,39].

$$I_0=1.3*Ms+0.09 \qquad (1)$$

$$I=11.926+(0.831*Ms)-2.7Ln(R+22) \qquad (2)$$

Where: Ms is surface magnitude, I_0 is intensity in epicenter, R is radius from epicenter and I is earthquake intensity in the specific place.

It is obvious that the results which were obtained from empirical attenuation relations, long as we consider the parameters influencing on the microzonation, could be helpful for evaluating effects of earthquake. Described parameters in subsection 3.1 are arranged systematically under engineering judgment of amplification coefficient of Tabriz city. After overlaying of parameters, a cell-by-cell ($10*10$ m^2) arithmetic combination (Eq. 3) gives amplitude map (Fig. 4b).

$$A_i=\sum G_i M_i T_i W_i S_i \qquad (3)$$

Where A_i is amplification map in area i; G_i is combination of geology and sedimentology map; M_i is microtremor measurements; T_i is alluvial thickness; W_i is ground water table and S_i is geoid slope values. The purpose of seismic analysis step is quantifying of earthquake ground shaking that may be experienced in the Tabriz metropolitan. Consequently, the ground shaking map (Fig. 5) is produced by combination of raw intensity map and amplitude map (Eq. 4).

$$GSM=\sum A_i I_i \qquad (4)$$

Table 3 Fault model elements of source earthquake.

NTF elements	Descriptions
Starting point in UTM coordinates (X,Y)	(624555.925,4213508.213)
Ending point in UTM coordinates (X,Y)	(584957.047,423450.388)
Reference point in UTM coordinates (X,Y)	(606924.994,422636.423)
Magnitude (M_w)	7
Length (km)	45
Strike (deg)	270
Dip (deg)	90

Where GSM is ground shaking map; A_i is Amplitude map; I_i is intensity map.

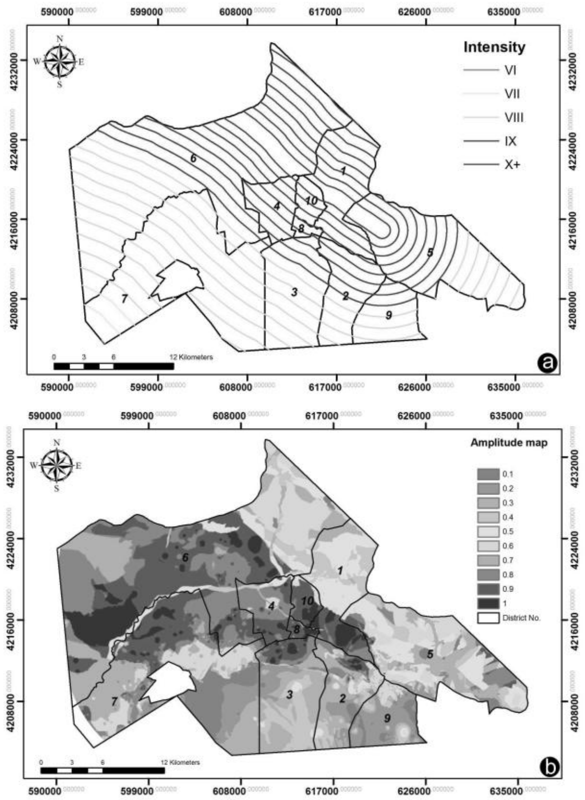

Fig 4. a, Intensity map of earthquake from a 7 magnitude earthquake (the roman numbers represent Modified Mercali Intensity); b, Seismic amplitude map.

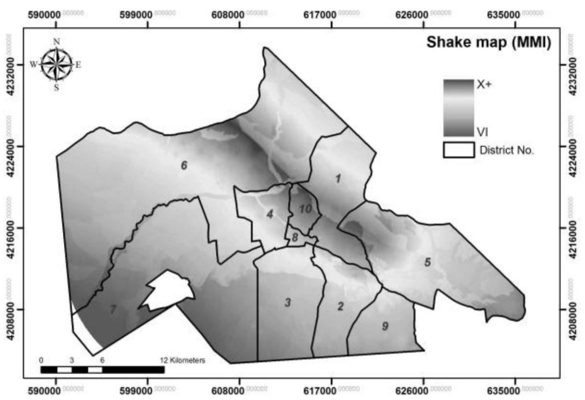

Fig 5. Ground shaking map illustrating the regional extend of intensity that can be expect from a 7 magnitude earthquake on the North Tabriz Fault.

(3) Vulnerability analysis

The word "vulnerability" is used to indicate the extent of damage that may be occurred to buildings, communities or each geographic feature. When an earthquake occurs, a city and its components, such as urban transportation, telecommunication network, households and buildings are exposed to destruction risk and loss of their functionalities. The complex urban systems are heavily related to each other and mostly their functionality depend on the other activities. Therefore, urban vulnerability is not only depending on a particular component or section of the city, but also the entire component all together.

On the other hand, must note that fatalities of large-scale earthquakes are mostly as a result of buildings collapses. Earthquake loss studies during the 20th century reveal that 75% of deaths have been caused by collapsed buildings in which people trapped or buried under rubbles and waste materials [40]. For this reason we take building types into consideration as a primary risk scenario to estimate building damage and consequently population vulnerability. Comparison of Manjil and Kocaeli earthquakes which happened in Iran and Turkey respectively revealed that Iranian buildings are 1 grade weaker than Turkey's buildings despite of the same magnitude of earthquakes [41]. JICA developed fragility curve functions for 8 different types of buildings to evaluate stability of buildings in Tehran [41-43]. Sun-dried brick and mud (adobe) buildings depict high damage potential which are abundant in villages and also it was anticipated reinforced concrete structures demonstrated the most acceptable performance in compared with steel of brick masonry structures (Fig. 6) [41]. This might be due to high integrity of structural elements in reinforced concrete structures such as foundations, columns, beams and slabs in comparison with the other types of structures. Building inventory provides only 5 building category for the study area, more precise damage/loss estimates require more extensive building inventory (i.e. time of construction, construction materials, lateral force-resisting system and quality). Only a few number of cities in the world have "well-developed" building inventories. In this study buildings type include: Brick-steel (60%), steel structure (33%), reinforced concrete building (4%) and cement block (1%) are building taxonomy of district two (Fig.8a). Damage ratio for each building determined based on Table 4.

Population vulnerability is one of the key categories of vulnerability analysis which is defined as the degree of population losses from a natural disaster such as earthquake. Population losses can be estimated by use of census tracts. In this study, we use 2006 census data which provided by Management and Planning Organization (Fig. 7). The total population in 10 districts is 1,189,989 people. The population of each census tract is divided equally to the number of residential units (parcels). As mentioned, night

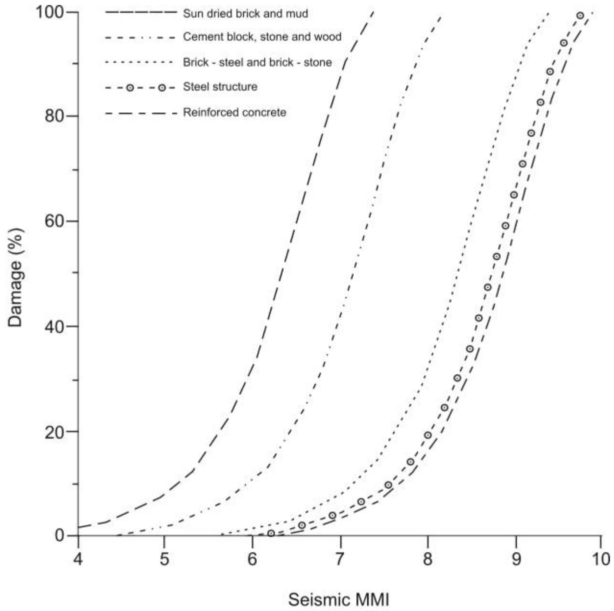

Fig 6. Fragility curves of 5 building types in the study region as a function of Modified Mercalli Intensity scale (MMI) [41].

Table 4 Description of building damage level adopted by Hassanzadeh et al., 2013[2] and corresponding damage level by EMS 1998 [43].

Destruction level	Damage percent	Descriptions
No destruction	0-2	Damages are underestimate
Light destruction	3-10	Very tiny cracks
Moderate destruction	11-30	5-20 mm cracks are seen in the building
High destruction	31-60	>20 mm cracks are seen and some components of building such as walls are destroyed
Very high destruction	61-80	A part of roof and one building's wall is destroyed
Totally destroyed	81-100	Entire of roof and more than one building's wall destroyed

earthquakes are dominant in this area therefore a worst-pessimistic scenario for night time is selected in order to estimate population vulnerability report (number of died, hospitalized injured and non-hospitalized population) of district two (Eq. 5).

$$H=\sum BP_i*PK_i \quad (5)$$

Where H is population vulnerability, BP_i is number of people in the buildings in each specific damaged zone and PK_i is probability of being (died, hospitalized injured, non-hospitalized and not injured) (Table 5).

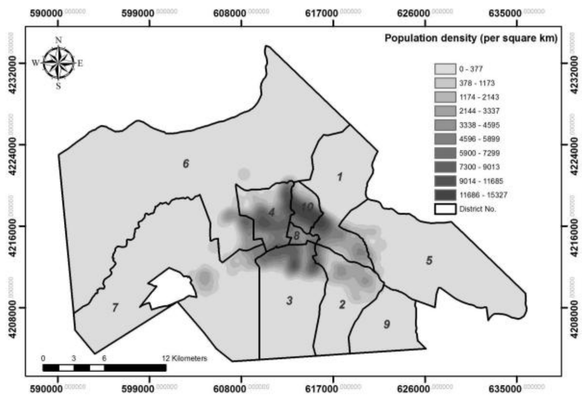

Fig 7. Population density of Tabriz city in 2006.

Table 5 Classification of expected population damage based on questionnaire surveys and reports of previous earthquakes in Iran [44].

Type of destruction	Status of people	Damage %
No destruction	Dead	0
	Hospitalized	0
	Non-hospitalized	1
	Not injured	99
Light destruction	Dead	2
	Hospitalized	5
	Non-hospitalized	9
	Not injured	84
Moderate destruction	Dead	4
	Hospitalized	9
	Non-hospitalized	15
	Not injured	72
High destruction	Dead	13
	Hospitalized	17
	Non-hospitalized	23
	Not injured	47
Very high destruction	Dead	16
	Hospitalized	22
	Non-hospitalized	28
	Not injured	34
Totally destroyed	Dead	41
	Hospitalized	16
	Non-hospitalized	21
	Not injured	22

4. RESULTS

The results based on GIS-oriented analysis indicate that 69.5% of the buildings as totally destroyed, 18% as very highly destroyed, 12% as highly destroyed and 0.5% as moderately destroyed (Fig. 8b). Overall, the area of district two is around 42.92 km^2 including parks, streets, alleys and vacant lands, and pure residential area is 6.8 km^2 which 3.1 km^2 is totally destroyed as a result of the simulated earthquake. The three-dimentional perspective of buildings before and after earthquake scenario in district two are shown in Fig. 9. As illustrated in Figure 9, most vulnerable structures are located in North and West parts of district two and majority of sturdy structures against the earthquake vibrations are located in the new towns (i.e. Yaghchian) of eastern boundary. Infirmaries as an important place after any disaster are damaged seriously (Fig. 8a,b) due to their poor constructions. 41% of infirmaries are collapsed totally and are not able to hinder against post-disasters.

Using the population dataset, building vulnerability results and population vulnerability ratios (Table 5) in different classes the population vulnerability report is estimated (Table 6) [44]. Survival inside trapped places usually last just for about 2 days after an earthquake therefore the number of rescuers or temporary infirmaries are crucial factors in the immediate aftermath of an earthquake. Basic demands after earthquake scenario are calculated based on KDMC [44] criteria and reported in Table 7.

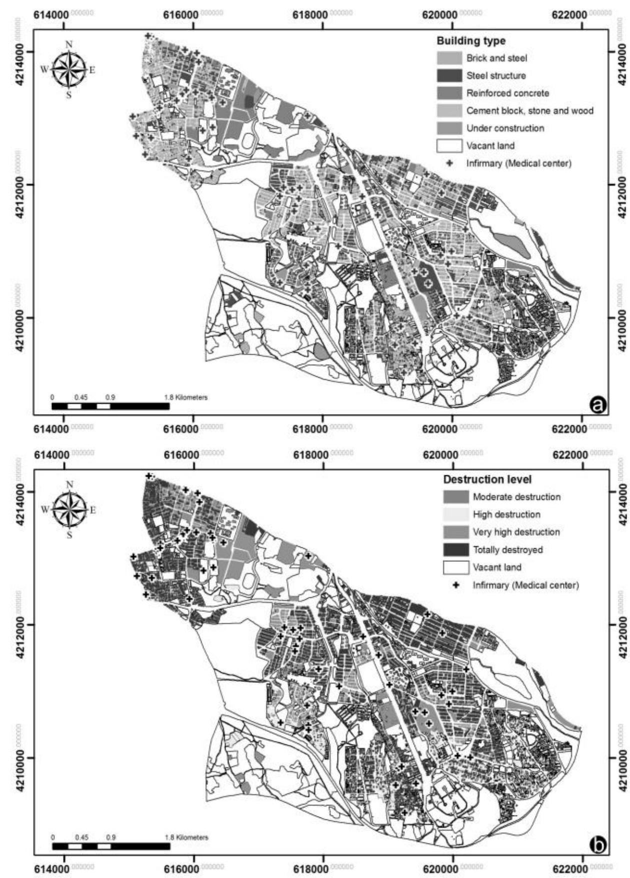

Fig 8. a, building types in district two; b, destruction map.

Table 6 Population vulnerability due to a M 7 earthquake.

Destruction level	Exposed population	Vulnerable population	Loss level
Totally destroyed	58167	23848	Dead
		9307	Hospitalized injured
		12215	Non-hospitalized
		12797	Not injured
Very high destruction	15233	2437	Dead
		3351	Hospitalized injured
		4265	Non-hospitalized
		5180	Not injured
High destruction	10178	1323	Dead
		1730	Hospitalized injured
		2341	Non-hospitalized
		4784	Not injured
Moderate destruction	7	0	Dead
		1	Hospitalized injured
		1	Non-hospitalized
		5	Not injured

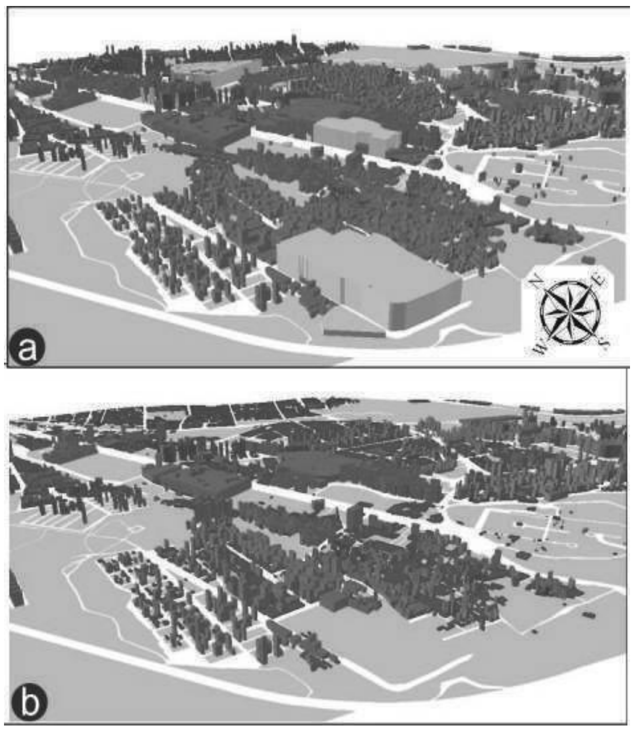

Fig 9. Three-dimensional view of the study area. a, before earthquake b, after earthquake.

Table 7 Estimated resources based on KDMC 2008 and Hassanzadeh et al. [2,44,45].

Material	The number of resources
Rescuer	5,598
Shovel	28,364
Emergency toilet	2,799
Emergency bath	2,799
Stick and splint	332,110
Bandage	332,110
Field infirmary	144
Drinking water bottle (/day)	167,931
Canned food (/day)	223,908
Bread pieces (/day)	111,954
Blanket	55,977

5. CONCLUSION

This paper presented a new microzonation map through a series of influential parameters. Parameters are converted to shape files, classified and finally integrated in a relational geodatabase. Microzonation map is produced by pixel-dependence overlaying of effective parameters. Delineation of seismic hazard zones requires establishing effective parameters which are clearly defined by their impacts in the seismic microzonation, urban planning and/or land management. For example feasibility of geoid slope map as an effective parameter in Iranian plateau has been applied. Seismic hazard zonation map then used to determine potential building damage in district two of Tabriz city in which exhibits lower hazards than other highly populated districts such as districts four, eight and ten. Minimum and maximum of the felt intensity in district two is IV and X, respectively. During the last centuries Tabriz city was growing across the hazardous area. Widespread damages and casualties due to earthquakes in 1721 (30000 people killed) and in 1780 (50000 people killed) in Tabriz city had not a profound effect on new urban revisions. This study demonstrated that brick-steel masonry buildings are mostly vulnerable buildings in district two probably due to disintegrating of the mortar and bricks. Even some old unreinforced masonry buildings in district two might be collapsed as a consequence of moderate earthquake occurrence. Therefore the attentions should be focused on feeblenesses in building construction, especially low quality materials which are not comply with building standard codes for earthquake-resistant design and the lack of proper supervision during the construction operations of private buildings.

ACKNOWLEDGEMENTS: The authors would like to express their gratitude to Dr. Abdolhossein Fallahi from Azarbaijan Shahid Madani University, Iran who prepared most required data. The financial support provided by the Kanazawa University, Japan.

REFERENCES

1) Kamel S. Crisis management of earthquake in pre-occurrence stage by using of GIS. Case study: Municipality of Tabriz region 1. University of Tabriz, Faculty of Geography. Master of Science thesis 2012.
2) Hassanzadeh R, Zorica N, Alavi Razavi A, Norouzzadeh M, Hodhodkian H. Interactive approach for GIS-based earthquake scenario development and resource estimation (Karmania hazard model). Computers & Geoscience 2013; 51: 324–338.
3) Prompt Assessment of Global Earthquakes for Response (PAGER). <http:// earthquake.usgs.gov/eqcenter/pager/S >; 2010.
4) Porter KA, Jaiswal K, Wald D.J, Hearne M. Developing loss models for the US Geological Survey's Prompt Assessment of Global Earthquakes for Response (PAGER) system. Proceedings of 14WCEE, Beijing, China 2008.
5) Erdik M, Şeşetyan K, Demircioğlu M.B, Hancılar U, Zülfikar C. Rapid earthquake loss assessment after damaging earthquakes. Soil Dynamics and Earthquake Engineering 2011; 31: 247–266.
6) FEMA, 2003a.HAZUSMH MR4 Earthquake Model User Manual. Department of Homeland Security. Federal Emergency Management Agency.Mitigation Division.Washington, D.C. 2012; www.fema.gov/library/viewRecord.do?id=3732.
7) FEMA, 2003b.HAZUSMH MR4 Earthquake Model Technical Manual. Department of Homeland Security.Federal Emergency Management Agency.Mitigation Division.Washington, D.C. 2012; www.fema.gov/library/viewRecord.do?id=3732.
8) Yuba County, Multi-Jurisdictional Multi-Hazard Mitigation Plan.http://www.co.yuba.ca.us.
9) FEMA, Harris County, Texas Uses HAZUS-Multi Hazard for Risk Assessment & Hurricane Preparedness.2005;http://www.fema.gov/hazus/harris-county-texas-uses-hazus-multi-hazard-risk-assessment-hurricane-preparedness.
10) Cinicioglu S.F, Bozbey I, Oztoprak S, Kelesoglu M.K. An integrated earthquake damage assessment methodology and its application for two districts in Istanbul, Turkey. Engineering Geology 2007; 94: 145–165.
11) Ansal A, Kurtulus A, Tonuk G. Seismic microzonation and earthquake damage scenarios for urban areas. Soil Dynamics and Earthquake Engineering 2010; 30: 1319–1328.
12) Armaş I. Multi-criteria vulnerability analysis to earthquake hazard of Bucharest, Romania. Natural Hazards 2012; 63: 1129–1156.
13) W. Cole S, Xu Y, W. Burton P. Seismic hazard and risk in Shanghai and estimationof expected building damage. Soil Dynamics and Earthquake Engineering 2008; 28: 778–794.
14) Hashemi M, Alesheikh A.A. A GIS-based earthquake damage assessment and settlement methodology. Soil Dynamics and Earthquake Engineering 2011; 31: 1607–1617.
15) Jackson J. Partitioning of strike-slip and convergent motion between Eurasia and Arabia in Eastern Turkey and the Caucasus.Journal of Geophysical Research 1992; 97 (B9), 12471–12479.

16) McClusky et al. (2000), GPS constraints on plate kinematics and dynamics in the eastern Mediterranean and Caucasus, Journal of Geophysical Research, 105: 5695–5719.
17) Westaway R. Block rotation in western Turkey 1. Observational evidence. Journal of Geophysical Research 1990; 95 (B12): 19857–19884.
18) McKenzie D.P, Active tectonics of the Mediterranean region. Geophysical Journal of Royal Astronomical Society 1972; 30: 109–185.
19) Toksöz M.N, Arpat E, Saroglu, F. East Anatolia earthquake of 24 November, 1976 Nature 1977; 270: 423–425.
20) Jackson J, McKenzie D. P. The relationship between plate motions and seismic moment tensors, and the rates of active deformation in the Mediterranean and the Middle East. Geophysical Journal International 1988; 93: 45–73.
21) Hessami Kh., Jamali F, Tabassi H. Major active faults of Iran: Tehran, Iran, International Institute of Earthquake Engineering and Seismology 2003; 1 sheet, scale 1:2,500,000.
22) Berberian M. Natural hazards and the first earthquake catalogue of Iran. International Institute of Earthquake Engineering and Seismology 1994; 1: 266–270.
23) Karimzadeh S, Cakir Z, Osmanoğlu B, Schmalzle G, Miyajima M, Amiraslanzadeh R, Djamour Y. Interseismic strain accumulation across the North Tabriz Fault (NW Iran) deduced from InSAR time series. Journal of Geodynamics 2013; 66: 53–58.
24) Dehghani G.A, and Makris J. The gravity field and crustal structure of Iran. Geological Survey of Iran 1983; 51: 51–68.
25) Tehran Padir Consulting Co. Tabriz seismic microzoation investigations 2006; Vol 1:42–60.
26) Nowroozi A.A. Empirical relations between magnitude and fault parameters for earthquakes in Iran. Bulletin of the Seismological Society of America 1985. 75: 1327–1338.
27) Wells D.L, Coppersmith K.J. New empirical relationships among magnitude, rupture length, rupture width, rupture area, and surface displacement. Bulletin of the Seismological Society of America 1994; 84: 974–1002.
28) Mohajer A, Nowroozi A.A. Observed and probable Intensity Zoning of Iran. Tectonophysics 1987; 49:21–30.
29) Bonilla M.G, Mark R.K, Lienkaemper J.J. Statistical relations among earthquake magnitude, surface rupture length, and surface fault displacement. Seismological Society of America Bulletin 1984; 74: 2379–2411.
30) Pazhouhesh Omran Rahvar Engineering Consultants. Interim report of geotechnical investigations of Tabriz Urban Railway project 2008.
31) Assadian O, Eftekharnejad J, Jalilian M, Afsharianzadeh A.M. Geology map of Tabriz region. Geological Survey of Iran. 1 sheet, scale 1:100,000.
32) Barthelmes F. Definition of Functionals of the Geopotential and Their Calculation from Spherical Harmonic Models 2013; http://icgem.gfz-potsdam.de/ICGEM.
33) Kiamehr R, Sjöberg L.E. Impact of a precise geoid model in studying tectonic structures—A case study in Iran. Journal of Geodynamics 2006; 42: 1–11.
34) Fallahi A, Erami M.H, Mashayekhi h.R, Miyajima M. Microtremor and Shear Wave Velocity Measurements in Tabriz to Use in Seismic Microzonation. 6th International Conference of Seismology and Earthquake Engineering 2011.
35) Abdolahi M.R, Jamali F, Pedrami M, Haddadan M, Ghaemi J, Ghomashi A. Engineering geological maps of Tabriz. Engineering (compressive strength, suspectibility to slide, discontinuity surface). Geological Survey of Iran. 1 sheet, scale 1:50,000.
36) Iranian code of practice for seismic resistance design of buildings. Iranian Building Codes and Standards, Standard No. 2800. 3rd edition. Building and Housing Research Center (BHRC) 1999.
37) Seismic Rehabilitation of Existing Buildings No.360. Management and Planning Organization 2007 (In Persian).
38) Chandra V, Mc Whorter J.G, Nowroozi A.A. Attenuation of Intensities in Iran. Bulletin of the Seismological Society of America 1979; 69: 237–250.
39) Siahkali Moradi A, Mirzaei N, Rezapour M. Attenuation relationships of seismic intensity in Iran. Journal of Earth and Space Physics 2004; 30: 1–9.
40) Coburn A, Spence R. Earthquake Protection. 2nd edition. West Sussex, England: John Wiley and Sons Ltd; 2002.
41) The Study on Seismic Microzoning of the Greater Tehran Area in the Islamic Republic of Iran. Final Report. Japan International Cooperation Agency (JICA) and Centre for Earthquake and Environmental Studies of Tehran (CEST) and Tehran Municipality 2000.
42) ATC-13 Earthquake Damage Evaluation Data for California. Applied Technology Council. Redwood city, CA 1985.
43) Grünthal G. European Macroseismic Scale 1998(EMS-98). Cahiers du Centre Europeen de Geodynamique et de Seismologie, Vol. 15. Centre Europeen de Geodynamique et de Seismologie, Luxembourg; 1998. p.99.
44) Karmania Hazard Model User Manual. Kerman Disaster Management Center (KDMC). Kerman, Iran 2008; p. 235.
45) Humanitarian Charter and Minimum Standards in Humanitarian Response (Sphere), Northampton, United Kingdom, The Sphere Project, Belmont Press Ltd; 2004.

(Received September 4 , 2013)